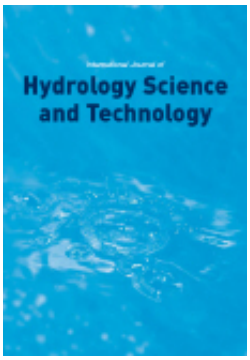

International Journal of Hydrology Science and Technology

ISSN online: 2042-7816 - ISSN print: 2042-7808
https://www.inderscience.com/ijhst

A framework for the evaluation of MRP complex precipitation in a CORDEX-SA regional climate applied to REMO

Shashikant Verma, A.D. Prasad, Mani Kant Verma

DOI: 10.1504/IJHST.2022.10049165

Article History:
Received: 03 September 2021
Accepted: 03 June 2022
Published online: 01 December 2023

A framework for the evaluation of MRP complex precipitation in a CORDEX-SA regional climate applied to REMO

Shashikant Verma*, A.D. Prasad and Mani Kant Verma

Civil Engineering Department,
National Institute of Technology,
Raipur, Chhattisgarh, India
Fax: +91-771-2254600
Email: shashiv50@gmail.com
Email: adprasadiit@gmail.com
Email: manikverma.ce@nitrr.ac.in
*Corresponding author

Abstract: In this study, rainfall patterns are depicted using 16 regional climate models of seasonal monsoon across the Mahanadi Reservoir Project (MRP) Complex region from 1980 to 2005. Bias correction and different statistical analyses were used to evaluate the model's degree of uncertainty and model performance with the relevant observations, respectively. The purpose of this study is to: 1) compare the capability of regional climate models (RCMs) in reproducing seasonal monsoons; 2) climate change impact in the near future (2021–2046), mid-future (2047–2072), and far-future (2073–2098) over the study area. The seasonal monsoon rainfall under two different RCPs (RCP 4.5 and 8.5) was used to test the experiments and data's ability. Among 16 Coordinated Regional Climatic Downscaling Experiment (CORDEX) models, the REgional MOdel (REMO 2009) has a higher R^2 (i.e., 0.610). Therefore, such studies assist to analyse the impact of monsoon rainfall on different sectors and responding to climate change.

Keywords: CORDEX-South Asia; MRP complex; regional climate model; RCM; bias correction; statistical analysis.

Reference to this paper should be made as follows: Verma, S., Prasad, A.D. and Verma, M.K. (2024) 'A framework for the evaluation of MRP complex precipitation in a CORDEX-SA regional climate applied to REMO', *Int. J. Hydrology Science and Technology*, Vol. 17, No. 1, pp.17–45.

Biographical notes: Shashikant Verma is a research scholar pursuing PhD from the National Institute of Technology, Raipur, India. He received his Bachelor's degree in Civil Engineering from the Professional Institute of Engineering and Technology, Raipur, and a Master's degree in Water resources Engineering from National Institute of Technology, Raipur. His current area of research interest is in water resource development and irrigation engineering, climate change, reservoir optimisation, time series modelling, hydrological modelling, and rainfall-runoff assessment.

A.D. Prasad is an employee of the National Institute of Technology, Raipur, India, and working as an assistant professor. He received his PhD degree in Geomatics Engineering from the Indian Institute of Technology Roorkee,

Uttarakhand. His current area of research interest is remote sensing, air pollution monitoring, remote sensing image fusion, image processing, medical image processing, geomatics engineering, and land surface temperature.

Mani Kant Verma is an employee of National Institute of Technology, Raipur, India and working, as an Assistant Professor. He received his Bachelors degree in Civil Engineering from G.B. Pant University of Agriculture and Technology, Pant Nagar, Uttarakhand and Master's degree in Water Resources and Environmental Engineering from Indian Institute of Science, Bangalore, Karnataka. His current area of research interest is in Water resources and environmental engineering, fluid mechanics, urban water distribution, system hydrology, optimisation techniques.

1 Introduction

For water assets, the data about water accessibility, water quality, and amount are of the most extreme significance for the present just as well as the future. Nearly every country in the world should foresee a net negative effect of environmental change on their water assets and biological freshwater systems. Precipitation is exceptionally uneven in space and time. The most elevated, rainfall-getting district on the planet is northeastern India, unlike the Thar Desert in western India. In contrast to the most recent 100 years, precipitation and temperature changes in India from 2000 to 2015 have been notable (Goyal and Surampalli, 2018). In comparison, the direct dangers of environmental change impact agribusiness, fisheries, health, and water protection in different regions of the world as well as the travel industry. Therefore, the preparation and monitoring of these events are essential for future strategy creation, supply operations, asset management, and environmental change assessments.

Climate models are essential for improving our understanding and consistency of conducting the atmosphere regularly on annual, decadal, and centennial time scales. Models are examining how often observed changes in the environment could be due to natural changeability, human activity, or a combination of both. Their outcomes and forecasts provide simple data to more readily educate choices about regional, local, and nearby importance, such as executive water properties, agribusiness, transportation, and urban planning. These days, numerous mainstream researchers are dynamically utilising different climate models to evaluate the Indian monsoon (Kumar et al., 2013). As a result, climate models are frequently employed to assess the existing and future effects of climate change on hydrology. The study of traditional climate–hydrology relationships serve as a guideline for future climate change scenarios and their implications for water resources development, making it increasingly important to make more reliable and exact predictions of climate variables (Smitha et al., 2018). Global and regional climate models (RCMs) are forerunners and powerful scientific tools for displaying climate and influencing environmental change assessments (Kumar and Dimri, 2018). The local models are tuned to speak to the present atmosphere as practically as could reasonably be expected to fabricate certainty for its ensuing use for tending to future projections under various environmental change scenarios.

A hindrance to the global climate models (GCMs) is their genuinely coarse horizontal resolution. For most impact studies, for example, assessment of flood risks or a few sorts of avalanches, dry seasons, and so forth, the general public requires data at a substantially more point-by-point nearby scale than given by GCMs. Hence, to examine climate assessments at a local scale, a high-resolution form of GCM is utilised, known as the RCM (Yang et al., 2020; Pastén-Zapata et al., 2020; Mendez et al., 2020; Laflamme et al., 2016). RCM is a supplement to GCM by further detailing global climate projections or contemplating atmospheric forms more detailed than GCMs permit. RCMs are created by settling a GCM into an RCM by utilising the horizontal boundary states of the GCM. RCMs are made through the dynamical downscaling of GCM yields (Seiler et al., 2018; Wu et al., 2017; Lucas-Picher et al., 2017; Prein et al., 2016; Eden et al., 2012). RCMs downscale GCMs to a resolution of 50 km or less to provide a fine-scale depiction of a local climate (Choudhary et al., 2018).

Recently, the Coordinated Regional Climatic Downscaling Experiment (CORDEX) project, an international collaborative effort, has given downscaled precipitation data for the past and future climate shifts, as well as a framework for evaluating models over East Asia (Giorgi et al., 2009). A number of prior studies have examined the performance of an individual RCM or an ensemble of RCMs in predicting East Asian precipitation patterns and extreme events (Huang et al., 2015; Park et al., 2016; Li et al., 2018). Extreme precipitation in China and East Asia has been replicated by RCMs despite systemic bias in mean and extreme precipitation (Park et al., 2016; Li et al., 2018).

As previously stated, the RCM model is employed in this study to downscale rainfall simulations over the CORDEX South Asia region. As a result, the RCM model outputs will be generated and referred to as ‘model scenario outputs’ in the future. The historical tests were carried out from 1980 to 2005, and the forecasts were carried out from 2006 to 2100 using Representative Concentration Pathways Scenarios (Van Vuuren et al., 2011a). The RCPs are the result of a novel combination of integrated assessment modellers, climate modellers, terrestrial ecosystem modellers, and emission inventory experts (Van Vuuren et al., 2011a). In this study, two RCP scenarios are used, which are called after the radiative forcing target level for 2100: RCP4.5 (Thomson et al., 2011) and RCP8.5 (Riahi et al., 2011). Towards the inner model domain, the global data is reduced exponentially as it approaches the domain’s lateral boundaries. Using a hybrid vertical coordinate system, the horizontal target resolution is 0.44 x 0.44 on a regular grid. The observed and predicted GHG concentration time series are fed into the regional historical and RCP simulations. In the regional experiments, ozone and aerosols are not taken into account, and natural climatic forces are constant (Fotso-Nguemo et al., 2017).

Many researchers have studied the CORDEX model ability to simulate rainfall characteristics. Mutayoba and Kashaigili (2017) examined CORDEX RCM ability to simulate rainfall patterns across Mbarali River basin and it is recommended that for the coming study, for impact studies, it is critical that the RCMs and their ensemble mean be corrected using bias correction techniques. Sannan et al. (2020) included 10 CORDEX-SA RCMs in the analysis; Rai et al. (2019) included 5 CORDEX-SA RCMs in the analysis; Saranya and Nair Vinish (2021) include 5 GCM-RCM combinations selected from CORDEX-SA datasets over a humid tropical river basin in Kerala, India. Now, in the present study, we have included all the CORDEX-SA ensembles available on the

CORDEX South Asia Database, CCCR, and IITM (http://cccr.tropmet.res.in/cordex/files/downloads.jsp). The list of CORDEX South Asia Experiments used in this study is presented in Table 1. Therefore, the main advantage of this study, it is an applied-based research work that tends to assess/examine MRP Complex, which on the other hand, reacts as a lifeline of the Chhattisgarh state. Furthermore, this technique/model output is more robust compared to others and could give satisfactory recommendations to the policy-makers and stakeholders associated with the water management and planning unit.

The detailed objective of this study is to:

1 Examine the ability of experiments and data to replicate the characteristics of summer monsoon precipitation in the MRP Complex region under two different greenhouse gas emission scenarios Representative Concentration Pathways 4.5 and RCP 8.5 throughout three-time scales (2021–2046), (2047–2072), and (2073–2098). The experiment of Coordinated Regional Climate Downscaling Experiments in South Asia (CORDEX-SA) is used to judge precipitation meteorology over the Mahanadi reservoir project complex, Chhattisgarh.

2 To investigate the potential precipitation variation over the baseline period using CORDEX climate data and performs a time series analysis of the simulated rainfall data from CORDEX.

3 To detect the change point of future RCM scenario.

4 To examine the magnitude and pattern of trend during 2021–2098.

The purpose of this work is to investigate the ability of the REMO model to capture fundamental meteorological phenomena, such as the monsoon rainfall, as well as to provide guidelines for the interpretation of climate change. This manuscript is provided as follows: Sections 2 and 3 explain the study area and data used. Section 4 describes the methodology adopted for the entire study. Section 5 addresses the discussion about how rainfall patterns may vary in the future climate along with change point detection as well as model comparison. Section 6 contains a conclusion.

2 Study area

The Mahanadi is a major river that originates in the Dhamtari region of Chhattisgarh and drains into the Bay of Bengal. From its source to its drainage into the Bay of Bengal, the overall river length is 851 kilometres (Sahu et al., 2021a; Verma et al., 2022b). The MRP complex is located in the upper Mahanadi basin (UMB), drained by the Sheonath River. The area of UMB is around 29,796.65 sq. km. The MRP Complex in UMB consists of 9 rain gauge stations that are shown in Figure 1. With summer temperatures of about 29ºC and winter temperatures of 21ºC, the climate in the Mahanadi River region is predominantly sub-tropical. Most of the precipitation is from July to September [800 to over 1200 mm] and less than 50 mm from January to February (Panda et al., 2013; Sahu et al., 2021b, 2021d; Dhiwar et al., 2022).

Figure 1 Study area map (see online version for colours)

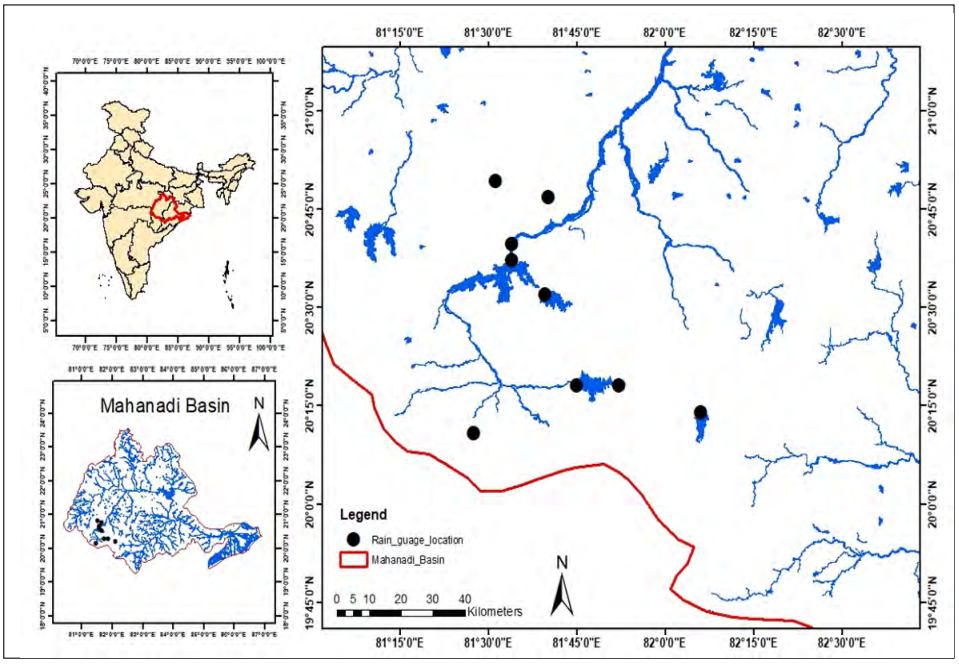

3 Data used

In the present study, in order to present the local climate change scenarios, the Coordinated Regional Climate Downscaling Experiment has been incorporated. They were funded by the World Climate Research Program to develop an improved version of local climate change projections for impact assessment and adaptation studies (Ghimire et al., 2018). Various modelling organisations worldwide have created the data structure for various experiments, consequently, their grid and structural format are distinct. The CORDEX vision is to progress and coordinate the science and use of regional climate downscaling through worldwide associations (Giorgi and Gutowski, 2015). The CORDEX RCM Simulations Precipitation Dataset is available on the Earth System and Grid Federation (ESGF) portal in NetCDF format, which is available on (https://esgf-data.dkrz.de/search/cordex-dkrz/) and a summary of RCMs used in this study is presented in Table 1. The water resource department of Chhattisgarh provides in-situ measurements that are used to evaluate the models. From 1980 to 2005, the daily precipitation measured at 13 meteorological stations was used (refer to Table 2). These meteorological stations are largely concentrated in the eastern part of the Mahanadi River basin, the MRP Complex region (see Figure 1). For data quality control, a standard normal homogeneity test is performed. This data is reliable and has been widely utilised to identify climate change and validate climate models.

Table 1 List of 16 CORDEX South Asia Experiments details

CORDEX-SA RCM	*RCM details*	*Influencing CMIP5 GCM*	*Acronyms*
IITM-RegCM4	The Abdus Salam International Centre for Theoretical Physics (ICTP) (Giorgi et al., 2012)	Centre for Climate Change Research (CCCR), Indian Institute of Tropical Meteorology (IITM), India	CanESM2 GFDL-ESM2M CNRM-CM5 MPI-ESM-MR IPSL-CM5A-LR CSIRO-Mk3.6
SMHI-RCA4	Rossby Centre regional atmospheric model version 4 (RCA4) (Jones et al., 2011)	Rossy Centre, Swedish Meteorological and Hydrological Institute (SMHI), Sweden	EC-EARTH MIROC5 HadGEM2-ES CanESM2 GFDL-ESM2M CNRM-CM5 MPI-ESM-LR IPSL-CM5A-MR CSIRO-Mk3.6
MPI-CSC-REMO 2009	MPI REgional MOdel (Teichmann et al., 2013)	Climate Service Center (CSC), Germany	MPI-ESM-LR

Source: CORDEX South Asia Database, CCCR, IITM http://cccr.tropmet.res.in/cordex/files/downloads. jsp

Table 2 Name of rain gauge stations and their locations

Stations	*Latitude (N)*	*Longitude (E)*
Birgudi	20.30	81.87
Chatti	20.78	81.67
Dudhawa	20.18	81.46
Gangrel	20.633	81.566
Dhamtari	20.822	81.522
Khajrawan Kanker	20.30	81.75
Murumsilli	20.533	81.666
Rudri	20.633	81.566
Sondur	20.233	82.10

4 Methodology

It is necessary to first topographically correct and then compares gridded simulations to the observations made at the observation stations. A number of statistical tests are used to analyse the correlation between simulated and observed results, including the Nash-Sutcliffe efficiency (NSE), root mean square error (RMSE), and the Taylor Diagram. The modified Mann-Kendall test is used to identify the trend pattern, and the

Pettit test is being used to examine the change point detection. Apart from that, the bias correction of climate models and methods used for bias correction techniques were discussed in Section 4.1 and the methodology flow chart is presented in Figure 2.

Figure 2 Methodology flow chart (see online version for colours)

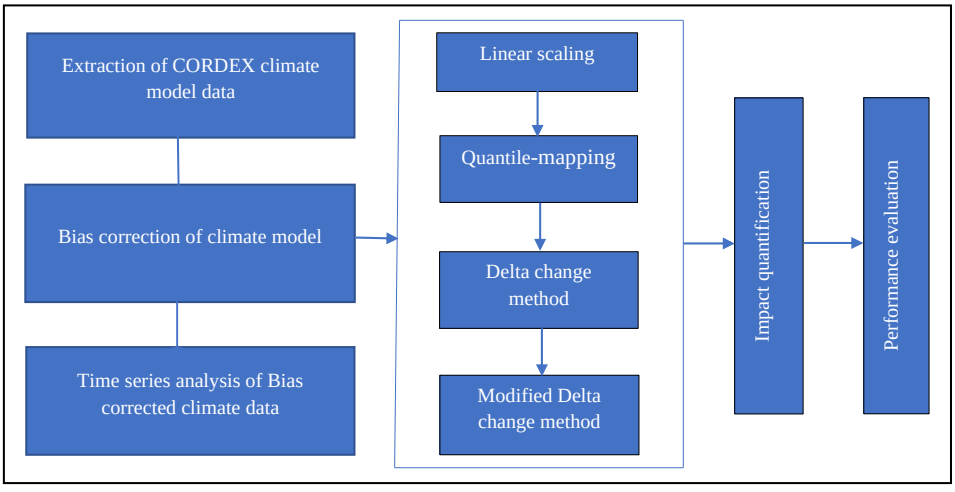

4.1 Bias correction of climate model

Biases are systemic errors caused by climate models and algorithms of estimation used in remote sensing i.e., inaccuracy within the system (Heo et al., 2019; Ehret et al., 2012). Broadly defined, bias can be described as the degree to which a mean forecast and a mean observation have an average correlation throughout time and space. Bias is used for an error in average precipitation. Bias is the proportional difference between the mean simulated output and the mean observed value over a given period. Here we focus on minimising or removing the bias of precipitation (Bennett et al., 2013). Mathematically expressed as:

$$B_R = \frac{R_{RCM} - R_{obs}}{R_{obs}} \times 100\% \tag{1}$$

B_R is biased, R_{RCM} is the mean precipitation of simulated model output, and R_{obs} is the mean of observed precipitation values. Often, when simulating the present-day atmosphere, compared to GCM forcing, in RCM, internal model processes are just as important as external ones, developing biases in climatological estimation (Gao et al., 2012). Examples of bias correction techniques include linear scaling, delta change method, modified delta change method, and quantile mapping (Gutmann et al., 2014).

4.1.1 Quantile mapping

It is a non-parametric bias correction technique. The statistical relationship between the simulated observed outputs and the model by replacing the simulated values with those observed at the same cumulative density function of the used distribution depends on the

climate variable (Cannon et al., 2015). Quantile mapping (QM) used a transfer function to compute the cumulative distribution function (CDF) of simulated model output and observed data, known as quantile mapping. Thus, the CDF of the corrected model is converted to match that of the data observed (Ayugi et al., 2020; Sahu et al., 2022). The QM is mathematically constructed as follows:

$$Y_m(t) = F_{obs}^{-1}\left[F_{RCM}\left\{Y_{RCM}(t)\right\}\right] \tag{2}$$

where $Y_m(t)$ is the bias-corrected data, $Y_{RCM}(t)$ is model-simulated data during some projected period and F_{RCM} and F_{obs}^{-1} the cumulative distribution function of RCM raw model data, is the inverse CDF (or quantile function) of the data observed.

The probability allocation of the concern variable for a future time is challenging to obtain. Future projected data is limited in evaluating climate change predictions (Gudmundsson et al., 2012). The quantile mapping approach has the advantage of representing RCM bias in every statistical moment. However, similar to all statistical downscaling approaches, it is assumed that bias related to observed historical data is consistent throughout the projections (Thrasher et al., 2012). For QM, the likelihood distribution models of observed and simulated data are necessary. Henceforth, it is important to choose a proper probability distribution model to implement the QM method effectively. The Gamma distribution has been utilised for the probability distribution of precipitation (Jeon et al., 2016).

The gamma distribution for precipitation used in this study is given by:

$$Y_m(t) = \begin{cases} F_{obs}^{-1}\left[F_{RCM}\left\{Y_{RCM}(t)\right\}\right], \left| Y_{RCM} \geq Y_{th} \right. \\ 0, \left| Y_{RCM} < Y_{th} \right. \end{cases} \tag{3}$$

Y is the climate variable; the threshold value of the wet and dry days is Y_{th}.

4.1.2 Linear scaling

The precipitation is a multiplicative correction that aims to match the model and observed data by correcting biases in the mean. It does not take into account biases in the variance, and the correction for rainfall is:

$$y_{\mathrm{mod},a,b} = y_{raw} - scen, a, b * \frac{\overline{y_{obs,b}}}{\overline{y_{raw,b}}} \tag{4}$$

where $y_{\mathrm{mod},a,b}$ is bias modified value of a^{th} day of b^{th} month, $y_{raw} - scen,a,b$ is the raw precipitation of scenario of a^{th} day of b^{th} month, $\overline{y_{obs,b}}$ is the mean of the observed value of precipitation of b^{th} month and $\overline{y_{raw,b}}$ is the mean of raw precipitation of b^{th} month.

4.1.3 Delta change method

It is a common method that is similar to linear scaling, except that the control period, called a 'hindcast', is put on top of the observational time series. This means that the control period affects the observational time series:

$$y_{raw} - hist, a, b = y_{obs,a,b} \tag{5}$$

$y_{obs,a,b}$ is observed time series of precipitation of a^{th} day of b^{th} month and $y_{raw} - h_{ist}$, a, b is the historical precipitation of the model corresponding to a^{th} day of b^{th} month. Then the bias-adjusted rainfall for a scenario is of the multiplicative form described below.

$$y_{\mathrm{mod},a,b} = y_{raw} - hist, a, b * \frac{\overline{y_{obs,b}}}{\overline{y_{raw,b}}} \tag{6}$$

4.1.4 Modified delta change method

A nonlinear transformation of historical precipitation data consists of the modified delta change method. The modified delta change method looks at changes in both average and extreme values to find the climate signal from climate model outputs. This is different from just looking at changes in the mean.

$$P^* = aP^b \text{ for, } P \le Q \tag{7}$$

$$P^* = aQ^b + E^F / E^C (P - Q) \text{ for, } P > Q \tag{8}$$

where Q is a large quantile, EC is the mean excess over the quantile Q in the Control climate and EF *is* the same for the future climate coefficients a and b following from future changes in, e.g., $P_{0.60}$ and $P_{0.90}$.

4.2 Performance of bias correction method

Statistical indices such as coefficient of determination (R^2) and Nash Sutcliffe efficiency (NSE) are used to evaluate the performance of the bias correction technique. The exactness of predictive models is essential because predictive models have been utilised across different disciplines, and predictive precision decides the quality of resultant predictions. Additionally, model execution is evaluated by comparing model values to observed values. In this study, it is inferred that REgional MOdel (REMO 2009) gives better simulations as compared to other RCMs.

4.3 Performance evaluations

For the evaluations of model performance certain statistical measures such as coefficient of determination (R^2), Nash Sutcliffe Efficiency (NSE), and RMSE are used and defined as follows:

4.3.1 Coefficient of determination

Examining statistical relationships between two variables is known as the Coefficient of Determination. It tells the linear relationship between two variables based on a correlation coefficient formula (Zhang, 2017).

$$(R^2) = \frac{n\left(\sum xy\right) - \left(\sum x\right)\left(\sum y\right)}{\sqrt{\left[n\sum x^2 - \left(\sum (x)^2\right)\right]}\sqrt{\left[n\sum y^2 - \left(\sum (y)^2\right)\right]}} \tag{9}$$

R^2 examines how another may explain discrepancies in one variable. The value of R^2 varies from 0 and 1. If the value of R^2 is equal to 1, then the data observed and the data from the model are perfectly balanced. If R^2 is 0, the correlation between observed and model data is weak.

4.3.2 Nash Sutcliffe efficiency

The correctness of model outputs can be evaluated using the Nash-Sutcliffe performance. Nash-Sutcliffe efficiency illustrates how well the 1:1 line fits the plot of observed results against simulations (McCuen et al., 2006). As illustrated in the following equation, Nash-Sutcliffe efficiency is calculated:

$$NSE = 1 - \frac{\sum_{i=1}^{n} (O_i - S_i)^2}{\sum_{i=0}^{n} (O_i - \bar{O})^2} \tag{10}$$

If O_i refers to observed data, S_i represents the simulated model output value, and $\bar{O}$ is the mean value of the observation data. The performance of NSE varies from $-\infty$ to 1. The closer to 1, the more precise the model. According to the model, the observed data mean is entirely consistent with the model predictions if NSE = 0, and If NSE > 0, the empirical mean is a stronger predictor.

4.3.3 Root mean square error

In order to determine the discrepancy between actual and predicted values, the RMSE is employed. The simulated or model data output is less than the RMSE value (Chai and Draxler, 2014). It is determined using the formula below:

$$RMSE = \sqrt{\frac{\sum_{i=1}^{n} (Y_i - X_i)}{n}} \tag{11}$$

where Y_i is the simulated data of the model and X_i is observed.

4.4 Time series analysis

This analysis is performed on the simulated data of CORDEX projections to understand the behaviour of the data. The simulated data has a span of 78 years, ranging from 2021 to 2098. The non-parametric statistics test is performed on data to observe its trend and change-point on an annual scale (Das et al., 2014; Verma et al., 2021). The test performed is the Modified Mann-Kendall Trend test to detect a trend and Sen's slope test for estimating the slope of the regression line along with Pettitt's change point test to detect the change in trend.

4.4.1 Modified Mann-Kendall test and Sen's slope estimator

The Modified Mann-Kendall test is a robust non-parametric test that can be used for all distributions. It can be used to identify long-term patterns in time-series data. The test works on two hypotheses: the null hypothesis (Ho) for this examination. The series does

not have a monotonic pattern, and the alternative hypothesis (Ha) is a trend. Positive, negative, or non-null may be the pattern. x_1, x_2, x_3, ..., xn the change version of Mann Kendall takes a look at which is strong within the autocorrelational relationship may exist, supported the changed variance of S is given by equation (12) and equation (14) (Hamed and Rao, 1998; Verma et al., 2022a; Sahu et al., 2021c).

$$Var(S) = E(S^2) = E\left[\sum i < j\, k < l\, S_{ij\ a_{kl}}\right] = \sum i < j\, k < l\, E_{(a_{ij} a_{kl})} \tag{12}$$

and $E_{(a_{ij} a_{kl})}$ is given by equation (13)

$$E_{(a_{ij}\ a_{kl})} = \frac{2}{\pi}\sin^{-1}\left(r_{ijkl}\right) \tag{13}$$

the variance (S) is given as:

$$V^*(S) = \text{var}(S)\cdot\frac{n}{n_S^*} = \frac{n(n-1)(2n+5)}{18}\frac{n}{n_S^*} \tag{14}$$

where $\frac{n}{n_S^*}$ is considered due to auto-correlation correction in the data and the statistically relevant pattern is calculated using the following test statistics:

$$Z = \begin{cases} \dfrac{S-1}{\sqrt{V^*(S)}} & if \quad S > 0 \\ 0 & if \quad S = 0 \\ \dfrac{S+1}{\sqrt{V^*(S)}} & if \quad S < 0 \end{cases} \tag{15}$$

A positive value (negative) of Z implies a pattern that is increasing (decreasing). Checking at a degree of significance, Ho is rejected for either an upward or downward monotonous trend. If Z is bigger than $Z_{1\text{-}\alpha/2,}$ as determined by the normal cumulative distribution tables. In addition, a simple non-parametric technique generated by Sen (1968) evaluated the magnitude of a time series pattern.

$$T = Median\left(\frac{x_j - x_i}{j-i}\right),\ j > I \tag{16}$$

where T is the Sen slope estimate. In the time series, $T > 0$ shows an upward trend. Otherwise, over time, the data series presents a downward trend.

4.4.2 Pettitt's change point tests

The methodology is generally used with continuous data to detect a change point in the hydrological or climate series. It tests the null hypothesis (Ho) (Pettitt, 1979; Azharuddin et al., 2022; Pradhan et al., 2022). A change-point exists in the P variables with the same position parameter after one or more distributions, against the alternate hypothesis (Ha). The non-parametric statistics are described as follows:

$$K_T = \max\left|U_{t,T}\right|, \tag{17}$$

$$U_{t,T} = \sum_{i=1}^{t} \sum_{j=t+1}^{T} Sgn\left(x_i - x_j\right) \tag{18}$$

If the statistics are relevant, the series change-point is K_T. K_T has approximated significance of 5% with,

$$p \cong 2\exp\left(\frac{-6\,K_T^2}{T^3 + T^2}\right) \tag{19}$$

5 Results and discussion

5.1 Results of RCMs

In the present study 16, CORDEX experiments were selected, and their ensemble and accompanying observations are plotted annually from 1980 to 2005, as shown in Figure 3. According to Figure 3, the REgional MOdel (REMO 2009) performs well as compared to other CORDEX climate models. However, the coefficient of determination for REgional MOdel (REMO 2009) is around 0.610, which is acceptable compared to other climate models (refer to Table 3). The same procedure applies to all rain gauge stations in the MRP Complex Region, Chhattisgarh, except the Dhamtari station coefficient of determination for REgional MOdel (REMO 2009) is around 0.665 (Refer to Table 3). Therefore, rest of the study, we choose the Dhamtari location as a reference station. The annual percentage change in observed rainfall is shown in Table 4. According to Table 4, the rainfall in a succeeding year is minimum for Dhamtari and Murumsilli around 3.55% and 2.88%, respectively whereas, Sondur and Birgudi stations have a maximum annual percentage change of rainfall i.e., 73.01 and 44.63.

Figure 3 The annual precipitation plot from the 16 CORDEX experiments, their ensembles, and related observations from 1980–2005 (see online version for colours)

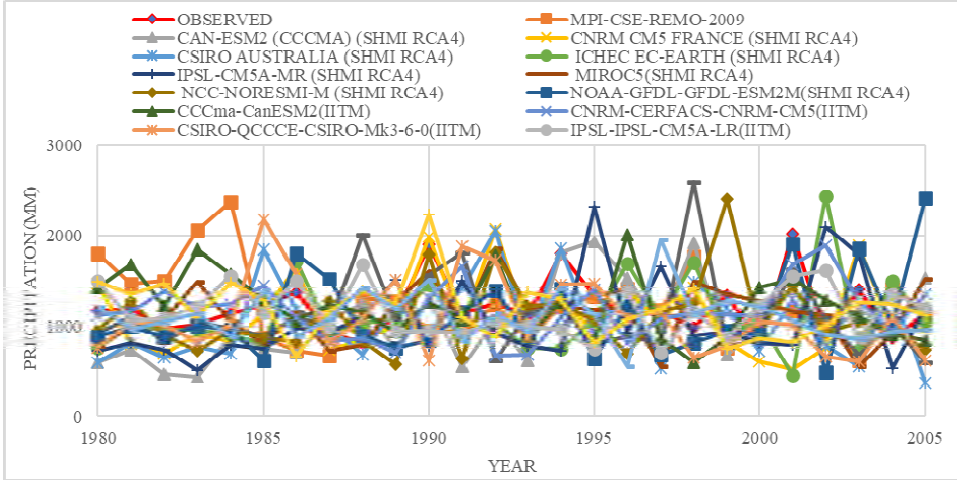

Table 3 Shows the coefficient of determination (R^2) of 16 CORDEX-SA climate models for the Dhamtari stations over the study region

Climate model	*Climate model group*	*(R^2)*	*Climate model*	*Climate model group*	*(R^2)*
MPI-ESM-LR	REMO	0.610	CanESM2	IITM-RegCM4)	0.469
CanESM2	SMHI-RCA4	0.332	CNRM-CM5		0.537
CNRM-CM5		0.481	CSIRO-Mk3.6		0.561
CSIRO-Mk3.6		0.336	IPSL-CM5A-LR		0.556
EC-EARTH		0.443	MPI-ESM-MR		0.536
IPSL-CM5A-MR		0.521	GFDL-ESM2M		0.530
MIROC5		0.456			
HadGEM2-ES		0.255			
MPI-ESM-LR		0.497			
NorESM1-M		0.379			

Table 4 Coefficient of determination (R^2) and annual percentage change of all the stations over the study region

Stations	*Annual percentage change (%)*	*Coefficient of determination (R^2)*
Birgudi	44.63765	0.090
Chhatti	38.14004	0.100
Dhamtari	3.553443	0.665
Dudhawa	36.05131	0.007
Gangrel	28.30453	0.629
Khajrawan Kanker	36.75524	0.151
Murumsilli	2.888521	0.166
Rudri	2.238775	0.018
Sondur	73.01632	0.161

5.2 Performance evaluations

As previously discussed in Section 5.1, REginoal MOdel (REMO 2009) performed well as compared to other CORDEX climate models as well as Dhamtari station is taken as a reference station for further studies which is having a higher coefficient of determination i.e., 0.665 as compared to other stations located in the study region. However, to remove the dissimilarities and uncertainties of model ensembles, four distinct bias-correction techniques were used. Therefore, to quantify the performance of such bias correction techniques three statistical analyses have been performed (refer to Table 5). As per Table 5, the Dhamtari station performs well in all four bias correction techniques as well as other stations located in the study region. Among four bias correction techniques modified delta change was performed exceptionally well in terms of error parameters and correlation coefficient, which is having $R^2 = 0.61$, NSE = 0.57, and RMSE = 95.75%. In addition, to quantify the performance of bias correction techniques Pearson correlation coefficient (PCC) was also assessed with the help of Taylor's diagram. According to Table 6, The modified delta change method performed well i.e., PCC = 0.826 as

compared to other methods (PCC = 0.781 for linear scaling, delta change method, and quantile mapping, respectively) for REgional MOdel (REMO 2009) and MPI-ESM-MR (IITM-RegCM4) ranked next where (PCC = 0.799, 0.781, 0.781, and 0.649 for modified delta change, linear scaling, delta change method, and quantile mapping, respectively) [see Figures 4(a), 4(b), 4(c), and 4(d)]. Furthermore, in the case of monthly precipitation for RCP 4.5 and RCP 8.5 scenarios, including a three-time slice showing maximum precipitation around 8000 mm from May to October for all the locations under MRP Complex region Chhattisgarh. Similarly, for seasonal precipitation, both scenarios have maximum rainfall of around 25,000 mm, including three-time scales, i.e., (2021–2046), (2047–2072), and (2073–2098), respectively (refer to Figure 5 to Figure 6). Figure 7(a), Figure 7(b) to Figure 8(a), Figure 8(b) represent a comparative study of observed precipitation before and after bias correction by Delta change, Linear scaling, Modified delta change, and Quantile mapping method, respectively for the Dhamtari station. From Figures 7(a), 7(b) to 8(a), 8(b) the modified delta change method performed well and satisfactory simulated the before and after bias correction concerning observed data in terms of both monthly and yearly time scales.

Figure 4 (a), (b), (c), and (d) Taylors diagram for Performance evaluation of South Asia CORDEX climate model precipitation using, (a) linear scaling (b) Delta change method (c) modified delta change method (d) quantile mapping for Dhamtari station under MRP Complex Region, Chhattisgarh (see online version for colours)

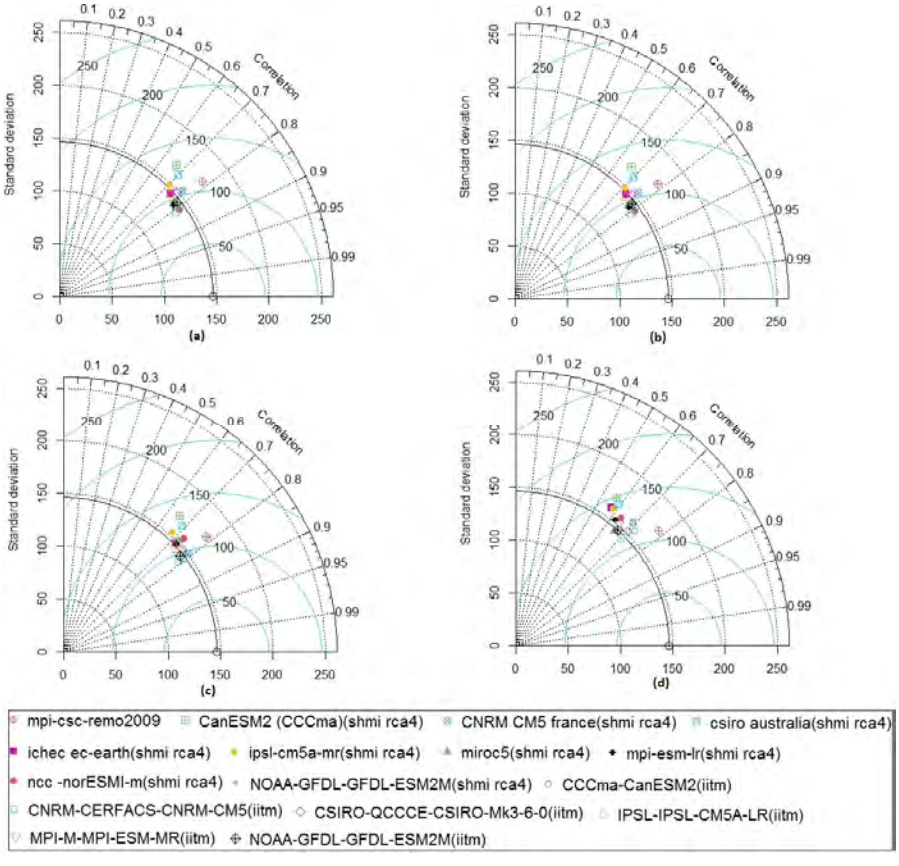

Table 5 Performance evaluation indices

Stations	*Linear scaling*			*Delta change*			*Modified delta change*			*Quantile mapping*		
	R^2	*NSE*	*RMSE*	R^2	*NSE*	*RMSE*	R^2	*NSE*	*RMSE*	R^2	*NSE*	*RMSE*
Birgudi	0.50	0.33	163.84	0.50	0.32	164.05	0.60	0.60	126.37	0.45	0.42	152.34
Chhatti	0.49	0.35	127.83	0.43	0.25	137.31	0.58	0.54	107.22	0.41	0.31	132.01
Dhamtari	0.51	0.36	116.91	0.50	0.35	117.11	0.61	0.57	95.78	0.61	0.26	109.52
Dudhawa	0.44	0.27	131.13	0.43	0.26	131.61	0.52	0.46	112.96	0.22	–0.04	156.99
Gangrel	0.34	0.07	140.74	0.49	0.33	119.34	0.60	0.56	96.68	0.59	0.39	114.13
Khajrawan Kanker	0.48	0.30	123.76	0.48	0.30	124.03	0.60	0.55	99.42	0.41	0.17	135.07
Murumsilli	0.49	0.35	129.82	0.49	0.35	130.12	0.58	0.54	109.29	0.44	0.31	133.90
Rudri	0.51	0.37	117.17	0.50	0.37	117.51	0.61	0.58	96.41	0.42	0.21	132.22
Sondur	0.44	0.23	130.66	0.44	0.23	130.92	0.57	0.52	102.88	0.45	0.12	139.38

Table 6 Pearson coefficient of Dhamtari station for 16 CORDEX climate models using four bias correction methods

Climate models	*Climate model group*	*Pearson correlation coefficient (PCC)*			
		Linear scaling	*Delta change*	*Modified delta change*	*Quantile mapping*
MPI-ESM-LR	REMO	0.781	0.781	0.826	0.781
CanESM2	SMHI-RCA4	0.664	0.664	0.578	0.565
CNRM-CM5		0.759	0.759	0.695	0.692
CSIRO-Mk3.6		0.70	0.70	0.582	0.592
EC-EARTH		0.731	0.731	0.667	0.572
IPSL-CM5A-MR		0.705	0.705	0.716	0.581
MIROC5		0.773	0.773	0.677	0.654
HadGEM2-ES		0.781	0.781	0.507	0.622
MPI-ESM-LR		0.809	0.809	0.707	0.637
NorESM1-M		0.775	0.775	0.617	0.588
CanESM2	IITM-RegCM4	0.80	0.80	0.686	0.722
CNRM-CM5		0.810	0.810	0.734	0.701
CSIRO-Mk3.6		0.750	0.750	0.751	0.701
IPSL-CM5A-LR		0.737	0.737	0.747	0.657
MPI-ESM-MR		0.782	0.782	0.799	0.649
GFDL-ESM2M		0.779	0.779	0.795	0.665

Table 7 Mann Kendall, Sen's slope, and Pettitt's test for all stations simulated by MPI-CSC-REMO 2009 CORDEX RCM for RCP 4.5 scenario

Stations	*Mann Kendall (P-value)*	*Sen's Slope (s)*	*Pettitt's test*	
			p-value	*Changepoint (t)*
Birgudi	0.979	–0.061	0.099	2081
Chatti	0.662	0.422	0.695	2081
Dhamtari	0.550	0.622	0.955	2081
Dudhawa	0.385	0.921	0.662	2039
Gangrel	0.483	0.737	0.699	2081
Khajrawan kanker	0.891	0.232	0.104	2081
Murumsilli	0.548	0.805	0.889	2081
Rudri	0.491	0.718	0.626	2081
Sondur	0.906	0.132	0.258	2036

Figure 5 Comparative study of observed monthly precipitation concerning RCP scenarios 4.5 and 8.5 in three different time scales for all the stations under MRP complex region, Chhattisgarh (see online version for colours)

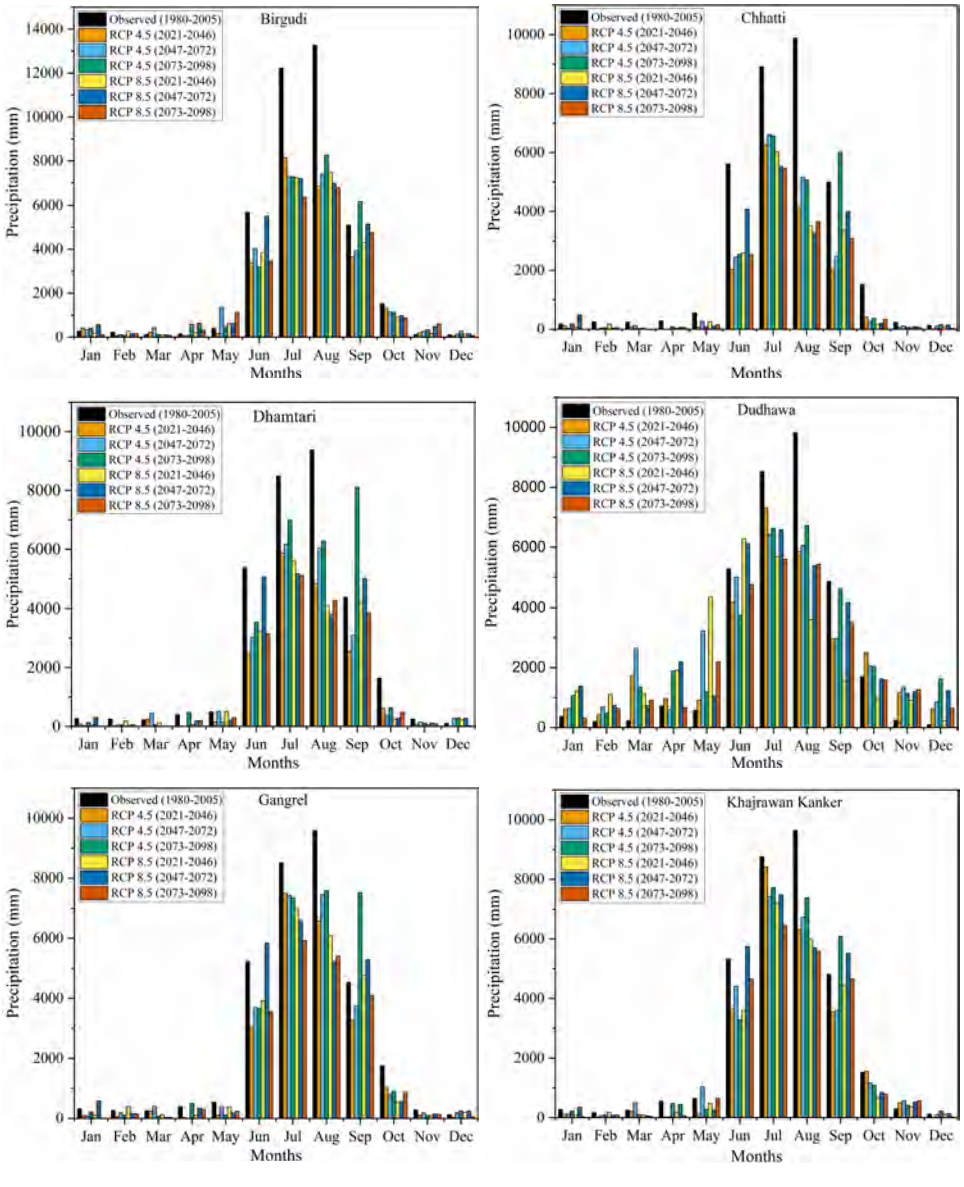

Figure 5 Comparative study of observed monthly precipitation concerning RCP scenarios 4.5 and 8.5 in three different time scales for all the stations under MRP complex region, Chhattisgarh (continued) (see online version for colours)

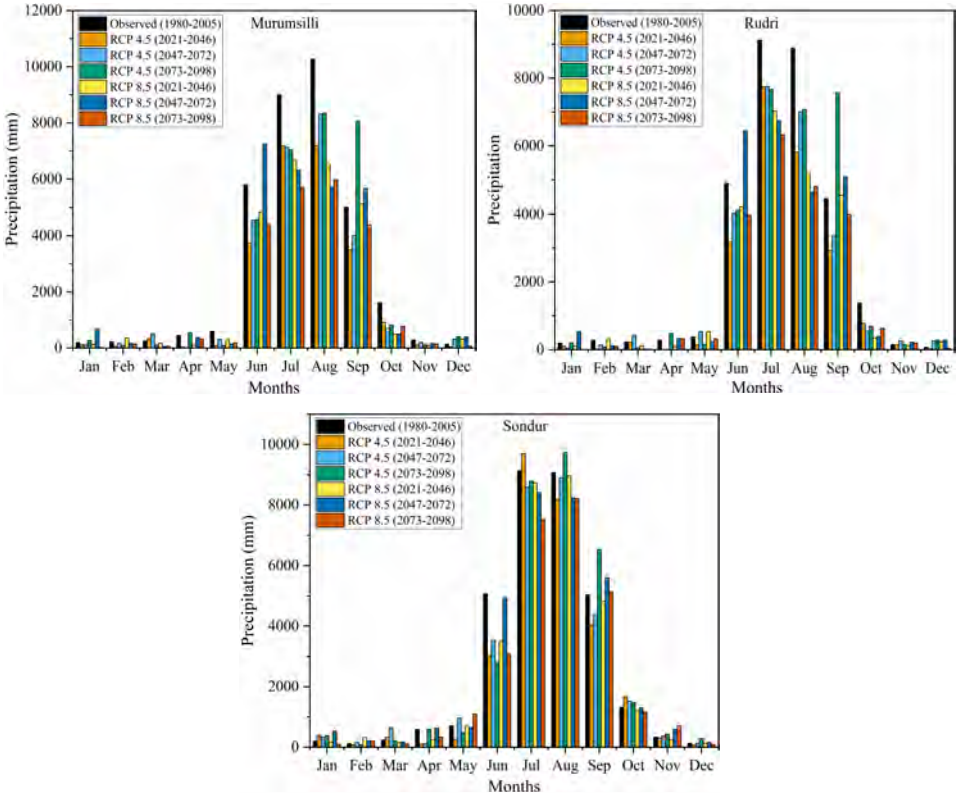

Table 8 Mann Kendall, Sen's slope, and Pettitt's test for all stations simulated by MPI-CSC-REMO 2009 CORDEX RCM for RCP 8.5 scenario

Stations	*Mann Kendall (P-value)*	*Sen's Slope (s)*	*Pettitt's test*	
			p-value	*Changepoint (t)*
Birgudi	0.032*	–2.340	0.054	2060
Chatti	0.018*	–2.667	0.018	2060
Dhamtari	0.038*	–2.464	0.033	2060
Dudhawa	0.122	–2.402	0.243	2060
Gangrel	0.034*	–2.696	0.024	2060
Khajrawan kanker	0.107	–2.154	0.104	2060
Murumsilli	0.051	–2.557	0.059	2060
Rudri	0.052	–2.732	0.078	2060
Sondur	0.028*	–2.942	0.025	2059

Figure 6 Comparative study of observed Seasonal precipitation concerning RCP scenarios 4.5 and 8.5 in three different time scales for all the stations under MRP complex region, Chhattisgarh (see online version for colours)

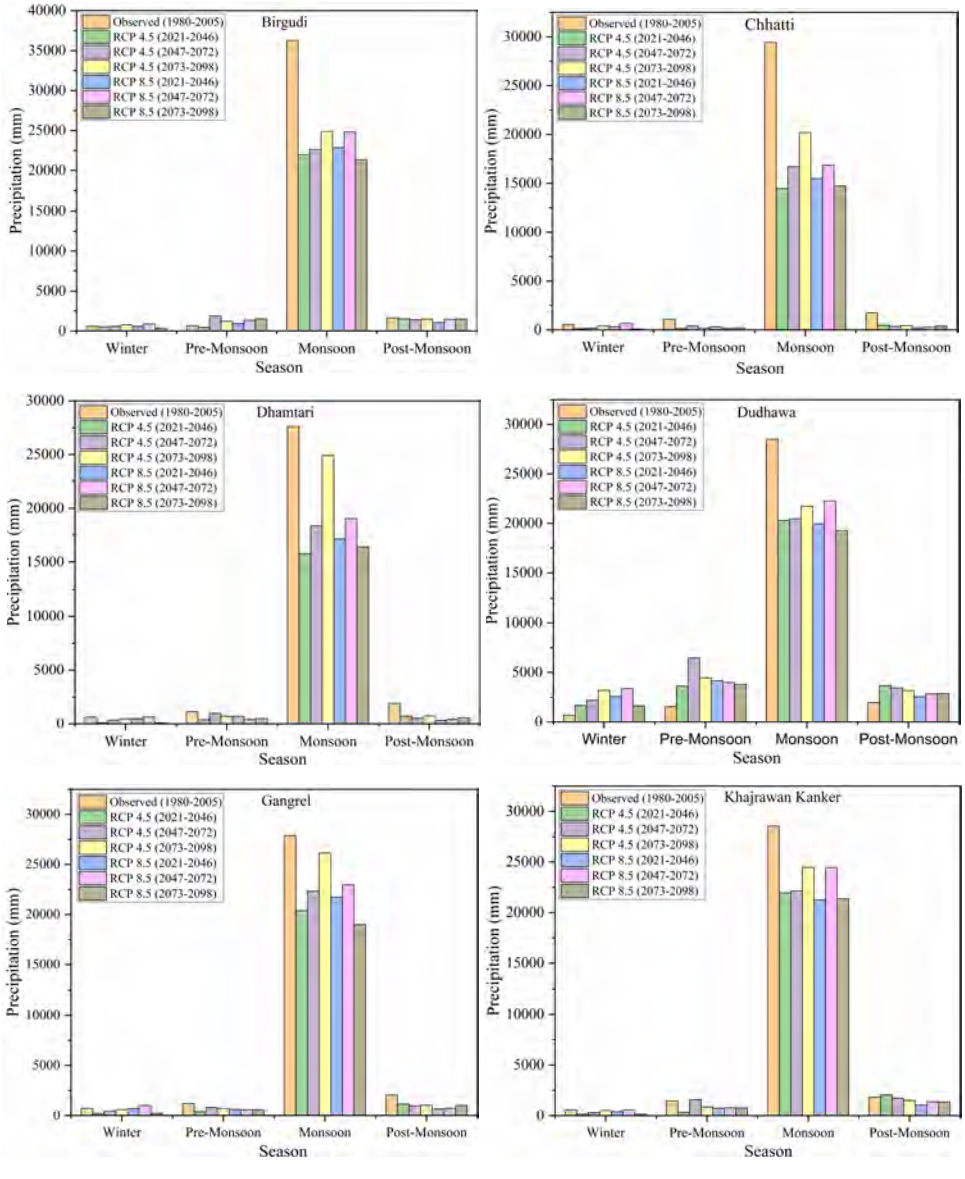

Figure 6 Comparative study of observed Seasonal precipitation concerning RCP scenarios 4.5 and 8.5 in three different time scales for all the stations under MRP complex region, Chhattisgarh (continued) (see online version for colours)

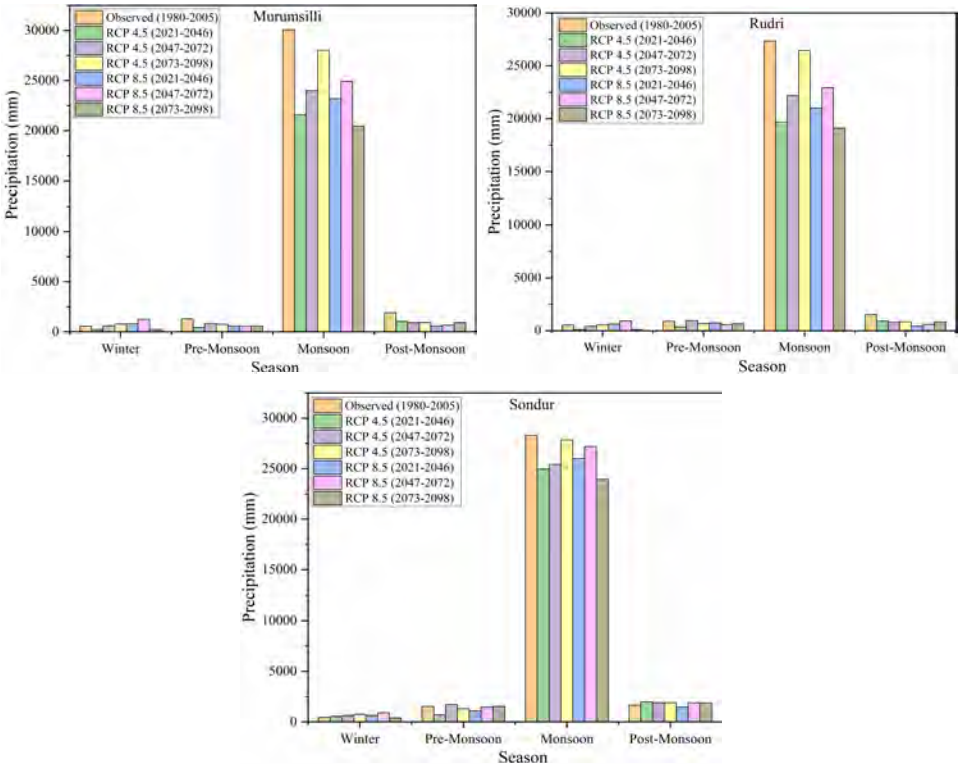

Figure 7 (a), (b) Comparative study of observed precipitation before Bias and after bias correction by, (a) Delta change method (b) linear scaling for monthly and yearly time scales of Dhamtari stations under MRP complex region, Chhattisgarh (see online version for colours)

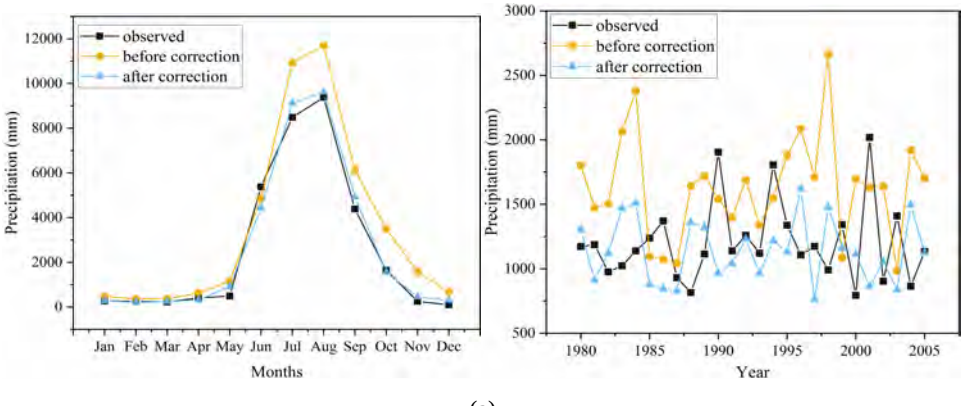

(a)

Figure 7 (a), (b) Comparative study of observed precipitation before Bias and after bias correction by, (a) Delta change method (b) linear scaling for monthly and yearly time scales of Dhamtari stations under MRP complex region, Chhattisgarh (continued) (see online version for colours)

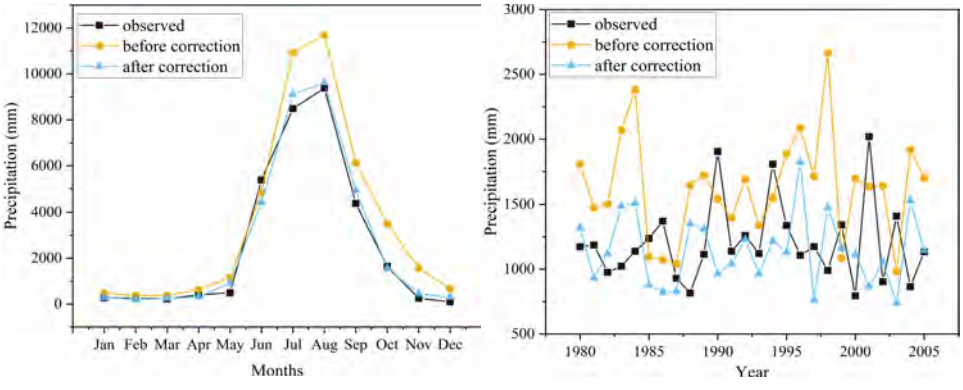

(b)

Figure 8 (a), (b) Comparative study of observed precipitation before Bias and after bias correction by (a) modified delta change method (b) quantile mapping for monthly and yearly time scales of Dhamtari stations under MRP complex region, Chhattisgarh (see online version for colours)

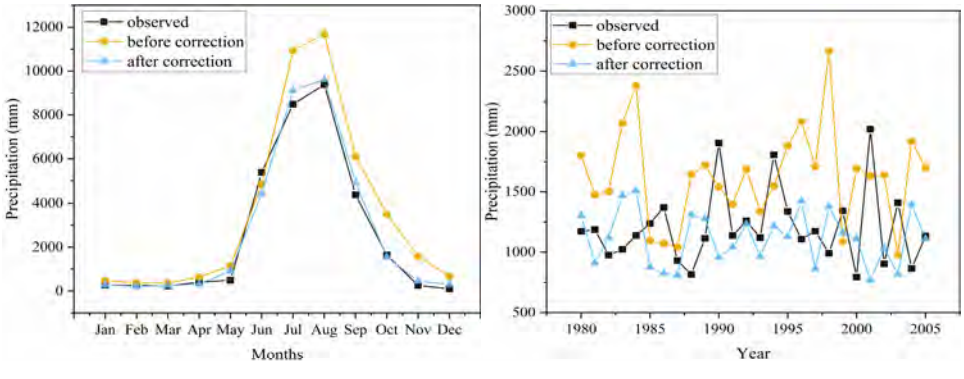

(a)

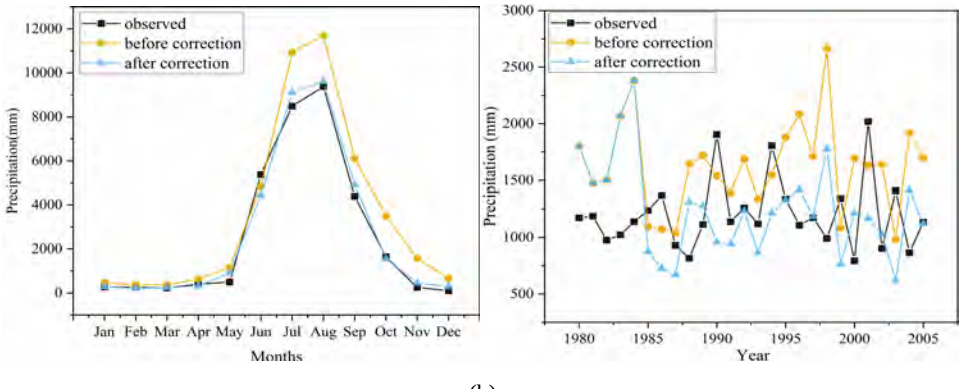

(b)

Table 9 Test statistics of monthly time scales of MPI-CSC-REMO (2021–2098) CORDEX RCM for all stations over the study region

Stations		*Jan*	*Feb*	*Mar*	*Apr*	*May*	*Jun*	*Jul*	*Aug*	*Sep*	*Oct*	*Nov*	*Dec*
Birgudi	MK	0.55	0.44	0.50	3.17	–0.025	0.17	–0.65	0.27	2.05	0.52	0.89	0.85
	SS	0	0	0	0	0	0	–0.53	0.24	0.88	0.07	0	0
	PV	0.57	0.65	0.61	0.001*	0.97	0.86	0.51	0.78	0.04	0.59	0.36	0.39
Chhatti	MK	0.61	0.87	–0.75	1.62	6.81	0.85	0.49	–0.11	2.17	0.59	1.73	1.80
	SS	0	0	0	0	0	0	0.30	–0.05	0.86	0	0	0
	PV	0.54	0.38	0.45	0.10	0.49	0.39	0.61	0.90	0.02*	0.55	0.08	0.07
Dhamtari	MK	1.80	0.61	0.87	–0.75	1.62	0.68	0.87	0.43	–0.09	2.16	0.59	1.73
	SS	0	0	0	0	0.10	0	0	0.25	0.92	1.08	0	0
	PV	0.07	0.54	0.38	0.45	0.490	0.49	0.38	0.66	0.04	0.03*	0.55	0.083
Dudhawa	MK	1.32	–0.26	0.60	0.98	–0.83	0.59	–0.46	–0.62	1.74	–0.36	0.48	–0.08
	SS	0	0	0	0	0	0.15	–0.3	–0.40	0.64	–0.10	0	0
	PV	0.18	0.18	0.54	0.32	0.40	0.55	0.64	0.53	0.08	0.71	0.62	0.93
Gangrel	MK	1.60	0.01	–0.09	1.91	0.79	0.44	–0.008	–0.17	2.54	0.49	0.76	0.64
	SS	0	0	0	0	0	0	–0.008	–0.14	1.43	0.03	0	0
	PV	0.10	0.98	0.92	0.05	0.42	0.65	0.99	0.86	0.01*	0.62	0.44	0.51
Khajrawan kanker	MK	0.26	1.07	0.20	1.58	0.74	0.76	–0.24	–0.54	1.59	–0.56	0.90	1.36
	SS	0	0	0	0	0	0	–0.24	–0.50	0.89	0	0	0
	PV	0.79	0.28	0.83	0.11	0.45	0.44	0.80	0.58	0.11	0.56	0.36	0.17
Murumsilli	MK	1.60	0.01	–0.07	1.91	0.79	0.48	0	–0.17	2.52	0.48	0.77	0.64
	SS	0	0	0	0	0	0	–0.004	–0.10	1.53	–0.02	0	0
	PV	0.10	0.98	0.93	0.05	0.42	0.62	1.0	0.86	0.01*	0.62	0.43	0.51
Rudri	MK	1.27	0.70	–0.22	1.86	0.66	0.73	0.04	0.004	2.20	0.67	1.08	1.13
	SS	0	0	0	0	0	0	0.07	0	1.19	0	0	0
	PV	0.20	0.48	0.82	0.06	0.50	0.46	0.96	0.99	0.02*	0.49	0.27	0.25
Sondur	MK	1.01	0.006	0.49	2.46	–0.95	1.90	–0.47	0.18	2.01	0.53	0.40	0.72
	SS	0	0	0	0	0	0	–0.43	0.19	0.99	0.11	0	0
	PV	0.30	0.99	0.62	0.01*	0.33	0.84	0.63	0.84	0.04*	0.59	0.68	0.46

Notes: Where MK stands for Mann-Kendall test statistics, SS stands for Sen slope, and PV stands for P-value whereas the '+ve' value depicts an increasing trend similarly '–ve' value depicts decreasing trend respectively and the asterisk *denotes a statistically significant trend at a 95% confidence level.

5.3 Results of trend analysis

REgional MOdel (REMO 2009) simulated annual rainfall patterns are summarised in Tables 7 to 8 for both RCP 4.5 and 8.5, respectively, for all stations in the study region from 2021 to 2098. As previously discussed in Section 4.4, the test was conducted with the help of Mann-Kendall statistics and Sen Slope estimator along with Pettitt's test to examine the change point detection on time series. According to Table 7, negative values depicts a decreasing trend, whereas positive values depicts an increasing one, whereas all the stations have an increasing trend with a magnitude of 0.921mm/year for Dudhawa station and Murumsilli ranked next (i.e., 0.805mm/year), except Birgudi station shows the decreasing trend with a magnitude of 0.061 mm/year along with consistent change point was observed in the year 2081 for all stations over the study region except Dudhawa and Sondur i.e., 2039 and 2036, respectively. Similarly, for the RCP 8.5 scenario, Table 8 shows the magnitude of the trend along with the occurrence of change point during 2021-2098, where the positive value demonstrates the increasing trend, the negative value depicts the decreasing trend, and the asterisk * stands for significant trend at 95% significance level. According to Table 8, all the stations in the study region show a 95% significant decreasing trend except Dudhawa, Khajrawan Kanker, Murumsilli, and Rudri. The maximum downward trend occurs with a magnitude of 2.942 mm/year for Sondur and 2.969 mm/year for Gangrel ranked next. In addition, the consistent change point was observed in the year 2060 for all stations over the study region except Sondur i.e., 2059.

A brief description of rainfall dependencies on a monthly time scale is presented in Table 9, asterisk * denotes a trend that is statistically significant at a 95% confidence level, while a positive value shows an increasing trend and a negative value shows a decreasing trend. For Birgudi, there is a year-round increasing trend with a magnitude of 3.17 mm/year in April, except for May and July, which show a decreasing trend with magnitudes of 0.97 mm/year and 0.51mm/year, respectively. Similarly, for Chatti, a significant increasing trend is seen in September with a magnitude of 0.86mm/year, except in March and August with a decreasing trend of 0.00mm/year and 0.05mm/year, respectively. In addition, in the case of the Dhamtari, the trend pattern is an increasing tendency throughout the year, with a substantial increase in October with a magnitude of 0.03 mm/year, except for April and September, which show a falling trend with a magnitude of 0 mm/year and 0.92 mm/year, respectively. In the case of Dudhawa, there is a decreasing trend throughout the year, except January, March, April, June, September, and November shows an increasing trend. There is no significant increase or decrease at this station (refer to Table 9). The trend pattern of Gangrel stations over the study region demonstrates that there is an upward trend throughout the year as well as a substantial upward trend with the magnitude of 1.43 mm/year for September. The months of March, July, and August show a downward trend. However, the trend pattern for Khajrawan Kanker indicates an increasing trend throughout the year, except for July, August, and October, which show a decreasing trend. It is very similar to the Khajrawan Kanker except for the September month, which exhibits a substantial increasing trend with a magnitude of 1.53 mm per year (mm/year). Apart from that, Rudri station shows an increasing trend throughout the year except for March and a substantial increase in September with a magnitude of 1.19 mm/year. Finally, the trend pattern for the Sondur station is increasing throughout the year at 0 mm/year and 0.99 mm/year for April and September, respectively. May and July show a decreasing trend (refer to Table 9). In

overall conclusion, an ensemble of RCMs simulates precipitation trends better than individual models. REgional MOdel (RCM 2009) produces the most realistic simulated trends among the 16 RCMs. A substantial model dependence on RCM simulation over the study region is indicated by large variances in simulated precipitation variations between different RCMs This illustrates that using a single RCM to assess climate change over a study region might be undertaken with prudence.

6 Conclusions

In this study, 16 CORDEX-SA RCMs were tested for their ability to simulate precipitation climatology from 1980 to 2005 over the study area. For this study, 16 RCMs were developed by SHMI and IITM, including the Rossby Centre regional atmospheric model (RCA4) and ICTP's Regional Climatic Model version 4.4.5 with a horizontal resolution of 0.440 (RegCM4), were compared to observational datasets. The RCA4 models and the ensemble are reviewed on a seasonal and annual basis for their performance. Additionally, several statistical metrics are used to ensure that the model's performance is robustly evaluated. Many different models and regions have been found to have vastly different performances. According to the findings of this study, earlier evaluations of the CORDEX's performance within the research area have provided valuable knowledge (Anyah et al., 2006; Endris et al., 2013). The study region consists of three major reservoirs: Ravishankar Sagar, Dudhawa, and Murumsilli, which supply water to around half of the Chhattisgarh state for irrigation, domestic, and industrial purposes. As a result, it is necessary to investigate summer monsoon precipitation across the MRP Complex region using CORDEX data to quantify future water availability. However, the performance of 16 CORDEX South Asia experiments and nine rain gauge stations in the study area was assessed for its capacity to capture and identify precipitation climatology from 1980 to 2005 over the MRP Complex region to reflect the current climate. This study was carried out in order to assess the output of each experiment and its ensembles. Concerning the corresponding observation, the efficiency of experiments was assessed. As observed from the uncertainty review, the experiments demonstrate a wide range of variability in replicating the precipitation over the study area, both in terms of time and space. However, in the overall sense, REgional MOdel (REMO 2009) shows better performance for the Dhamtari station for both RCP 4.5 and RCP 8.5 than individual experiments as well as other rain gauge stations. RCMs have a tendency to exhibit biases over the world in complex geography. These biases may be exaggerated because the measurements have inaccuracies and uncertainties because of the lack of dense observational networks. Compared with other experiments and their proximity to the observational dataset, only one experiment, REgional MOdel (REMO 2009), was selected because of better results. An observational dataset was used to demonstrate the experiments' overall performance throughout space and time. Therefore, the present study assesses the capabilities of different RCMs before employing them in a future ensemble forecast of climate change over the study region. In the future, more RCM simulations with higher resolution should be done and put together to learn more about how the climate of the study region changes.

Acknowledgements

The authors express their gratitude to the former CORDEX coordinate body and CMIP5 committee, the World Climate Research Program's Working Group on Regional Climate, and the Working Group on Coupled Modelling. I also thank the Earth System & Grid Federation (ESGF) and the Indian Institution of Tropical Meteorology (IITM) for rendering CORDEX South Asia data accessible. The authors thank NIT Raipur for its computational resources and other logistical support.

References

Anyah, R.O., Semazzi, F.H. and Xie, L. (2006) 'Simulated physical mechanisms associated with climate variability over Lake Victoria basin in East Africa', *Monthly Weather Review*, Vol. 134, No. 12, pp.3588–3609, https://doi.org/10.1175/MWR3266.1

Ayugi, B., Tan, G., Ruoyun, N., Babaousmail, H., Ojara, M., Wido, H., Mumo, L., Ngoma, N.H., Nooni, I.K. and Ongoma, V. (2020) 'Quantile mapping bias correction on rossby centre regional climate models for precipitation analysis over Kenya, East Africa', *Water*, Vol. 12, No. 3, p.801, https://doi.org/10.3390/w12030801.

Azharuddin, M., Verma, S., Verma, M.K. and Prasad, A.D. (2022) 'A synoptic-scale assessment of flood events and ENSO—streamflow variability in Sheonath River Basin, India', in *Advanced Modelling and Innovations in Water Resources Engineering*, pp.93–104, Springer, Singapore, DOI: 10.1007/978-981-16-4629-4_8.

Bennett, J.C., Grose, M.R., Corney, S.P., White, C.J., Holz, G.K., Katzfey, J.J., Post, D.A. and Bindoff, N.L. (2014) 'Performance of an empirical bias-correction of a high-resolution climate dataset', *International Journal of Climatology*, Vol. 34, No. 7, pp.2189–2204, https://doi.org/10.1002/joc.3830.

Cannon, A.J., Sobie, S.R. and Murdock, T.Q. (2015) 'Bias correction of GCM precipitation by quantile mapping: how well do methods preserve changes in quantiles and extremes?', *Journal of Climate*, Vol. 28, No. 17, pp.6938–6959, https://doi.org/10.1175/JCLI-D-14-00754.1.

Chai, T. and Draxler, R.R. (2014) 'Root mean square error (RMSE) or mean absolute error (MAE)? Arguments against avoiding RMSE in the literature', *Geoscientific Model Development*, Vol. 7, No. 3, pp.1247–1250, https://doi.org/10.5194/gmd-7-1247-2014.

Choudhary, A., Dimri, A.P. and Maharana, P. (2018) 'Assessment of CORDEX-SA experiments in representing precipitation climatology of summer monsoon over India', *Theoretical and Applied Climatology*, Vol. 134, No. 1, pp.283–307, https://doi.org/10.1007/s00704-017-2274-7.

Das, P.K., Chakraborty, A. and Seshasai, M.V. (2014) 'Spatial analysis of temporal trend of rainfall and rainy days during the Indian Summer Monsoon season using daily gridded (0.5×0.5) rainfall data for the period of 1971–2005', *Meteorological Applications*, Vol. 21, No. 3, pp.481–493, https://doi.org/10.1002/met.1361.

Dhiwar, B.K., Verma, S. and Prasad, A.D. (2022) 'Identification of flood vulnerable area for Kharun River Basin by GIS Techniques', in *Advanced Modelling and Innovations in Water Resources Engineering*, pp.385–408, Springer, Singapore, DOI: 10.1007/978-981-16-4629-4_27.

Eden, J.M., Widmann, M., Grawe, D. and Rast, S. (2012) 'Skill, correction, and downscaling of GCM-simulated precipitation', *Journal of Climate*, Vol. 25, No. 11, pp.3970–3984, https://doi.org/10.1175/JCLI-D-11-00254.1.

Ehret, U., Zehe, E., Wulfmeyer, V., Warrach-Sagi, K. and Liebert, J. (2012) 'HESS opinions' should we apply bias correction to global and regional climate model data?', *Hydrology and Earth System Sciences*, Vol. 16, No. 9, pp.3391–3404, https://doi.org/10.5194/hess-16-3391-2012.

Endris, H.S., Omondi, P., Jain, S., Lennard, C., Hewitson, B., Chang'a, L., Awange, J.L., Dosio, A., Ketiem, P., Nikulin, G. and Panitz, H.J. (2013) 'Assessment of the performance of CORDEX regional climate models in simulating East African rainfall', *Journal of Climate*, Vol. 26, No. 21, pp.8453–8475, https://doi.org/10.1175/JCLI-D-12-00708.1.

Fotso-Nguemo, T.C., Vondou, D.A., Tchawoua, C. and Haensler, A. (2017) 'Assessment of simulated rainfall and temperature from the regional climate model REMO and future changes over Central Africa', *Climate Dynamics*, Vol. 48, No. 11, pp.3685–3705, https://doi.org/10.1007/s00382-016-3294-1.

Gao, Y., Fu, J.S., Drake, J.B., Liu, Y. and Lamarque, J.F. (2012) 'Projected changes of extreme weather events in the eastern United States based on a high resolution climate modeling system', *Environmental Research Letters*, Vol. 7, No. 4, p.044025, https://doi.org/10.1088/1748-9326/7/4/044025.

Ghimire, S., Choudhary, A. and Dimri, A.P. (2018) 'Assessment of the performance of CORDEX-South Asia experiments for monsoonal precipitation over the Himalayan region during present climate: part I', *Climate Dynamics*, Vol. 50, No. 7, pp.2311–2334, https://doi.org/10.1007/s00382-015-2747-2.

Giorgi, F. and Gutowski Jr., W.J. (2015) 'Regional dynamical downscaling and the CORDEX initiative', *Annual Review of Environment and Resources*, Vol. 40, pp.467–490, https://doi.org/10.1146/annurev-environ-102014-021217.

Giorgi, F., Coppola, E., Solmon, F., Mariotti, L., Sylla, M.B., Bi, X., Elguindi, N., Diro, G.T., Nair, V., Giuliani, G. and Turuncoglu, U.U. (2012) 'RegCM4: model description and preliminary tests over multiple CORDEX domains', *Climate Research*, Vol. 52, pp.7–29, https://doi.org/10.3354/cr01018.

Giorgi, F., Jones, C. and Asrar, G.R. (2009) 'Addressing climate information needs at the regional level: the CORDEX framework', *World Meteorological Organization (WMO) Bulletin*, Vol. 58, No. 3, p.175.

Goyal, M.K. and Surampalli, R.Y. (2018) 'Impact of climate change on water resources in India', *Journal of Environmental Engineering*, Vol. 144, No. 7, p.04018054, https://doi.org/10.1061/(ASCE)EE.1943-7870.0001394.

Gudmundsson, L., Bremnes, J.B., Haugen, J.E. and Skaugen, T.E. (2012) 'Downscaling RCM precipitation to the station scale using quantile mapping–a comparison of methods', *Hydrology & Earth System Sciences Discussions*, Vol. 9, No. 5, pp.6185–6201, doi:10.5194/hessd-9-6185-2012.

Gutmann, E., Pruitt, T., Clark, M.P., Brekke, L., Arnold, J.R., Raff, D.A. and Rasmussen, R.M. (2014) 'An intercomparison of statistical downscaling methods used for water resource assessments in the United States', *Water Resources Research*, Vol. 50, No. 9, pp.7167–7186, https://doi.org/10.1002/2014WR015559.

Hamed, K.H. and Rao, A.R. (1998) 'A modified Mann-Kendall trend test for autocorrelated data', *Journal of Hydrology*, Vol. 204, Nos. 1–4, pp.182–196, https://doi.org/10.1016/S0022-1694(97)00125-X.

Heo, J.H., Ahn, H., Shin, J.Y., Kjeldsen, T.R. and Jeong, C. (2019) 'Probability distributions for a quantile mapping technique for a bias correction of precipitation data: a case study to precipitation data under climate change', *Water*, Vol. 11, No. 7, p.1475, https://doi.org/10.3390/w11071475.

Huang, B., Polanski, S. and Cubasch, U. (2015) 'Assessment of precipitation climatology in an ensemble of CORDEX-East Asia regional climate simulations', *Climate Research*, Vol. 64, No. 2, pp.141–158, https://doi.org/10.3354/cr01302.

Jeon, S., Paciorek, C.J. and Wehner, M.F. (2016) 'Quantile-based bias correction and uncertainty quantification of extreme event attribution statements', *Weather and Climate Extremes*, Vol. 12, pp.24–32, https://doi.org/10.1016/j.wace.2016.02.001.

Jones, C.G., Samuelsson, P. and Kjellström, E. (2011) 'Regional climate modelling at the Rossby Centre', *Tellus A: Dynamic Meteorology and Oceanography*, Vol. 63, No. 1, pp.1–3, https://doi.org/10.1111/j.1600-0870.2010.00491.x.

Kumar, D. and Dimri, A.P. (2018) 'Regional climate projections for Northeast India: an appraisal from CORDEX South Asia experiment', *Theoretical and Applied Climatology*, Vol. 134, No. 3, pp.1065–1081, https://doi.org/10.1007/s00704-017-2318-z.

Kumar, P., Wiltshire, A., Mathison, C., Asharaf, S., Ahrens, B., Lucas-Picher, P., Christensen, J.H., Gobiet, A., Saeed, F., Hagemann, S. and Jacob, D. (2013) 'Downscaled climate change projections with uncertainty assessment over India using a high resolution multi-model approach', *Science of the Total Environment*, Vol. 468, pp.S18–S30, https://doi.org/10.1016/j.scitotenv.2013.01.051.

Laflamme, E.M., Linder, E. and Pan, Y. (2016) 'Statistical downscaling of regional climate model output to achieve projections of precipitation extremes', *Weather and Climate Extremes*, Vol. 12, pp.15–23, https://doi.org/10.1016/j.wace.2015.12.001.

Li, H., Chen, H., Wang, H. and Yu, E. (2018) 'Future precipitation changes over China under 1.5 C and 2.0 C global warming targets by using CORDEX regional climate models', *Science of the Total Environment*, Vol. 640, pp.543–554, https://doi.org/10.1016/j.scitotenv.2018.05.324.

Lucas-Picher, P., Laprise, R. and Winger, K. (2017) 'Evidence of added value in North American regional climate model hindcast simulations using ever-increasing horizontal resolutions', *Climate Dynamics*, Vol. 48, No. 7, pp.2611–2633, https://doi.org/10.1007/s00382-016-3227-z.

McCuen, R.H., Knight, Z. and Cutter, A.G. (2006) 'Evaluation of the Nash–Sutcliffe efficiency index', *Journal of Hydrologic Engineering*, Vol. 11, No. 6, pp.597–602, https://doi.org/10.1061/(ASCE)1084-0699(2006)11:6(597).

Mendez, M., Maathuis, B., Hein-Griggs, D. and Alvarado-Gamboa, L.F. (2020) 'Performance evaluation of bias correction methods for climate change monthly precipitation projections over Costa Rica', *Water*, Vol. 12, No. 2, p.482, https://doi.org/10.3390/w12020482.

Mutayoba, E. and Kashaigili, J.J. (2017) 'Evaluation for the performance of the CORDEX regional climate models in simulating rainfall characteristics over Mbarali River catchment in the Rufiji Basin, Tanzania', DOI: 10.4236/gep.2017.54011.

Panda, D.K., Kumar, A., Ghosh, S. and Mohanty, R.K. (2013) 'Streamflow trends in the Mahanadi River basin (India): Linkages to tropical climate variability', *Journal of Hydrology*, Vol. 495, pp.135–149, https://doi.org/10.1016/j.jhydrol.2013.04.054.

Park, C., Min, S.K., Lee, D., Cha, D.H., Suh, M.S., Kang, H.S., Hong, S.Y., Lee, D.K., Baek, H.J., Boo, K.O. and Kwon, W.T. (2016) 'Evaluation of multiple regional climate models for summer climate extremes over East Asia', *Climate Dynamics*, Vol. 46, No. 7, pp.2469–2486, https://doi.org/10.1007/s00382-015-2713-z.

Pastén-Zapata, E., Jones, J.M., Moggridge, H. and Widmann, M. (2020) 'Evaluation of the performance of Euro-CORDEX Regional Climate Models for assessing hydrological climate change impacts in Great Britain: a comparison of different spatial resolutions and quantile mapping bias correction methods', *Journal of Hydrology*, Vol. 584, p.124653, https://doi.org/10.1016/j.jhydrol.2020.124653.

Pettitt, A.N. (1979) 'A non-parametric approach to the change-point problem', *Journal of the Royal Statistical Society: Series C (Applied Statistics)*, Vol. 28, No. 2, pp.126–135, https://doi.org/10.2307/2346729.

Pradhan, D., Sahu, R.T. and Verma, M.K. (2022) 'Flood inundation mapping using GIS and Hydraulic model (HEC-RAS): a case study of the Burhi Gandak river, Bihar, India', in Kumar R., Ahn, C.W., Sharma, T.K., Verma, O.P. and Agarwal, A. (Eds.): *Soft Computing: Theories and Applications, Lecture Notes in Networks and Systems*, Vol. 425, pp.135–145, Springer, Singapore, https://doi.org/10.1007/978-981-19-0707-4_14.

Prein, A.F., Gobiet, A., Truhetz, H., Keuler, K., Goergen, K., Teichmann, C., Fox Maule, C., Van Meijgaard, E., Déqué, M., Nikulin, G. and Vautard, R. (2016) 'Precipitation in the EURO-CORDEX $ $0.11^{\circ} $$0.11º and $ $0.44^{\circ} $$0.44º simulations: high resolution, high benefits?', *Climate Dynamics*, Vol. 46, No. 1, pp.383–412, https://doi.org/10.1007/s00382-015-2589-y.

Rai, P., Choudhary, A. and Dimri, A.P. (2019) 'Future precipitation extremes over India from the CORDEX-South Asia experiments', *Theoretical and Applied Climatology*, Vol. 137, No. 3, pp.2961–2975, https://doi.org/10.1007/s00704-019-02784-1.

Riahi, K., Rao, S., Krey, V., Cho, C., Chirkov, V., Fischer, G., Kindermann, G., Nakicenovic, N. and Rafaj, P. (2011) 'RCP 8.5—A scenario of comparatively high greenhouse gas emissions', *Climatic Change*, Vol. 109, No. 1, pp.33–57, https://doi.org/10.1007/s10584-011-0149-y.

Sahu, R.T., Verma, M.K. and Ahmad, I. (2021a) 'Some non-uniformity patterns spread over the lower Mahanadi River Basin, India', *Geocarto International*, pp.1–23, https://doi.org/10.1080/10106049.2021.2005699.

Sahu, R.T., Verma, M.K. and Ahmad, I. (2021b) 'Segmental variability of precipitation in the Mahanadi River Basin during 1901-2017', DOI: https://doi.org/10.21203/rs.3.rs-542786/v1.

Sahu, R.T., Verma, M.K. and Ahmad, I. (2021c) 'Regional frequency analysis using L-moment methodology – a review', in Pathak, K.K., Bandara, J.M.S.J. and Agrawal, R. (Eds.): *Recent Trends in Civil Engineering. Lecture Notes in Civil Engineering*, Vol. 77, Springer, Singapore, pp.811–832, https://doi.org/10.1007/978-981-15-5195-6_60.

Sahu, R.T., Verma, M.K. and Ahmad, I. (2021d) 'Characterization of precipitation in the sub-divisions of the Mahanadi River basin, India', *Acta Scientific Agriculture*, Vol. 5, No. 12, pp.50–61, https://doi.org/10.31080/ASAG.2021.05.1085.

Sahu, R.T., Verma, M.K. and Ahmad, I. (2022) 'Testing some grouping methods to achieve a low error quantile estimate for high resolution (0.25° x 0.25°) precipitation data', *J. Phys.: Conf. Ser.*, 2273 012017, https://doi.org/10.1088/1742-6596/2273/1/012017.

Sannan, M.C., Nageswararao, M.M. and Mohanty, U.C. (2020) 'Performance evaluation of CORDEX-South Asia simulations and future projections of northeast monsoon rainfall over south peninsular India', *Meteorology and Atmospheric Physics*, Vol. 132, No. 5, pp.743–770, https://doi.org/10.1007/s00703-019-00716-2.

Saranya, M.S. and Nair Vinish, V. (2021) 'Evaluation and selection of CORDEX-SA datasets and bias correction methods for a hydrological impact study in a humid tropical river basin, Kerala', *Journal of Water and Climate Change*, Vol. 12, No. 8, pp.3688–3713, https://doi.org/10.2166/wcc.2021.139.

Seiler, C., Zwiers, F.W., Hodges, K.I. and Scinocca, J.F. (2018) 'How does dynamical downscaling affect model biases and future projections of explosive extratropical cyclones along North America's Atlantic coast?', *Climate Dynamics*, Vol. 50, No. 1, pp.677–692, https://doi.org/10.1007/s00382-017-3634-9.

Sen, P.K. (1968) 'Estimates of the regression coefficient based on Kendall's tau', *Journal of the American Statistical Association*, Vol. 63, No. 324, pp.1379–1389, DOI: 10.1080/01621459.1968.10480934.

Smitha, P.S., Narasimhan, B., Sudheer, K.P. and Annamalai, H. (2018) 'An improved bias correction method of daily rainfall data using a sliding window technique for climate change impact assessment', *Journal of Hydrology*, Vol. 556, pp.100–118, https://doi.org/10.1016/j.jhydrol.2017.11.010.

Teichmann, C., Eggert, B., Elizalde, A., Haensler, A., Jacob, D., Kumar, P., Moseley, C., Pfeifer, S., Rechid, D., Remedio, A.R. and Ries, H. (2013) 'How does a regional climate model modify the projected climate change signal of the driving GCM: a study over different CORDEX regions using REMO', *Atmosphere*, Vol. 4, No. 2, pp.214–236, https://doi.org/10.3390/atmos4020214.

Thomson, A.M., Calvin, K.V., Smith, S.J., Kyle, G.P., Volke, A., Patel, P., Delgado-Arias, S., Bond-Lamberty, B., Wise, M.A., Clarke, L.E. and Edmonds, J.A. (2011) 'RCP4. 5: a pathway for stabilization of radiative forcing by 2100', *Climatic Change*, Vol. 109, No. 1, pp.77–94, https://doi.org/10.1007/s10584-011-0151-4.

Thrasher, B., Maurer, E.P., McKellar, C. and Duffy, P.B. (2012) 'Bias correcting climate model simulated daily temperature extremes with quantile mapping', *Hydrology and Earth System Sciences*, Vol. 16, No. 9, pp.3309–3314, https://doi.org/10.5194/hess-16-3309-2012.

Van Vuuren, D.P., Edmonds, J., Kainuma, M., Riahi, K., Thomson, A., Hibbard, K., Hurtt, G.C., Kram, T., Krey, V., Lamarque, J.F. and Masui, T. (2011a) 'The representative concentration pathways: an overview', *Climatic Change*, Vol. 109, No. 1, pp.5–31, https://doi.org/10.1007/s10584-011-0148-z.

Verma, S., Prasad, A.D. and Verma, M.K. (2021) 'Trend analysis and rainfall variability of monthly rainfall in Sheonath River Basin, Chhattisgarh', in *Recent Trends in Civil Engineering*, pp.777–790, Springer, Singapore, DOI: 10.1007/978-981-15-5195-6_58.

Verma, S., Prasad, A.D. and Verma, M.K. (2022a) 'Trends of rainfall and temperature over Chhattisgarh during 1901–2010', in *Advanced Modelling and Innovations in Water Resources Engineering*, pp.3–19, Springer, Singapore, DOI: 10.1007/978-981-16-4629-4_1.

Verma, S., Sahu, R.T., Prasad, A.D. and Verma, M.K. (2022b) 'Development of an optimal operating policy of multi-reservoir systems in Mahanadi Reservoir Project Complex, Chhattisgarh', *Journal of Physics: Conference Series*, May, Vol. 2273, No. 1, p.012020, IOP Publishing, http://dx.doi.org/10.1088/1742-6596/2273/1/012020.

Wu, C., Liu, X., Lin, Z., Rhoades, A.M., Ullrich, P.A., Zarzycki, C.M., Lu, Z. and Rahimi-Esfarjani, S.R. (2017) 'Exploring a variable-resolution approach for simulating regional climate in the Rocky Mountain region using the VR-CESM', *Journal of Geophysical Research: Atmospheres*, Vol. 122, No. 20, pp.10–939.

Yang, X., Yu, X., Wang, Y., He, X., Pan, M., Zhang, M., Liu, Y., Ren, L. and Sheffield, J. (2020) 'The optimal multimodel ensemble of bias-corrected CMIP5 climate models over China', *Journal of Hydrometeorology*, Vol. 21, No. 4, pp.845–863, https://doi.org/10.1175/JHM-D-19-0141.1

Zhang, D. (2017) 'A coefficient of determination for generalized linear models', *The American Statistician*, Vol. 71, No. 4, pp.310–316, https://doi.org/10.1080/00031305.2016.1256839.